

## Possibility of superluminal behaviors for *X*-like and Zenneck waves

A. Ranfagni and D. Mugnai

*Istituto di Ricerca sulle Onde Elettromagnetiche "Nello Carrara," CNR, Via Panciatichi 64, 50127 Firenze, Italy*

(Received 23 June 1998)

The possibility of observing superluminal behavior, in phase and group velocities, over distances of several wavelengths is demonstrated at the microwave scale, where we obtained evidence of *X*-like waves, and is discussed for the radio frequencies (Zenneck waves). [S1063-651X(98)10311-2]

PACS number(s): 03.40.Kf, 41.20.Jb, 73.40.Gk

### I. INTRODUCTION

Superluminal effects for evanescent modes have been demonstrated and interpreted in a number of tunneling experiments both in the optical domain and in the microwave range [1–5]. What clearly emerges from these works is that the group delay in crossing a barrier — whose width is of the order of the wavelength — is considerably shorter than the time employed by traveling at the light speed in vacuum. This implies that this effect can be revealed over short distances: in the case of microwaves these distances are of the order of a few centimeters. The question as to whether it is possible to extend these effects over larger distances naturally arises: the purpose of the present work is indeed to investigate such a possibility.

In a recent paper [6], Saari and Reivelt reported the experimental evidence of *X*-shaped localized light waves in a centimeter range — a notable one given the smallness of the optical wavelength — thus demonstrating a practical way of obtaining these kinds of waves, that have been theoretically predicted since the 1980s [7] and even before, especially in connection with their superluminal behavior [8]. We have reported results relative to anomalous short-delay in microwave propagation [9] and we interpreted them within the framework of a complex wave model. In Sec. II we report the salient features of the complex wave model together with the results of an experiment connected with complex waves, in close analogy with the *X*-shaped wave propagation. The possibility of extending this kind of investigation to the domain of radio frequencies (Zenneck waves [10]) is considered in Sec. III.

### II. COMPLEX WAVE MODEL AND *X*-LIKE WAVES

Let us consider the field emitted in the half-space  $\xi > 0$  from an aperture [in a conducting plane  $(\eta, \zeta)$ ] defined as infinite along  $\zeta$  and of finite size along  $\eta$ . According to the steepest-descent representation [11], the field can be expressed by adopting the same notations as in Ref. [9], with a contour integral in the complex plane of  $z = x + iy$  angle as

$$\int_C A(z) \exp[ik\rho \cos(z - \alpha)] dz, \quad (1)$$

where  $A(z)$  is the amplitude,  $\rho$  and  $\alpha$  are the polar coordinates of the observation point ( $\xi = \rho \cos \alpha$ ,  $\eta = \rho \sin \alpha$ ), and  $k = 2\pi/\lambda$  is the wave number. The original integration path

$([-\pi/2 + i\infty, -\pi/2]; [-\pi/2, \pi/2]; [\pi/2, \pi/2 - i\infty])$  is deformed into the steepest-descent path, which is given by the descending branch of the equation

$$\cos(x - \alpha) \cosh y = 1, \quad (2)$$

which crosses the real axis at the observation angle  $z = \alpha$ . If  $A(z)$  has poles at  $\beta$ 's angles situated (depending on  $\alpha$ ) inside the path deformation, the solution to the integral (1) must take the pole contributions into account, thus giving rise to complex waves. The solution to the integral can be therefore expressed as a superposition of a cylindrical wave (the "normal" contribution), of the  $A(\alpha) \sqrt{\lambda/\rho} \exp[i(k\rho - \pi/4)]$  type, and a sum of the pole contributions of the type [9]

$$2\pi i \bar{A}(\beta) \exp[ik\rho \cos(\beta_r - \alpha) \cosh \beta_i] + k\rho \sin(\beta_r - \alpha) \sinh \beta_i, \quad (3)$$

where  $\bar{A}(\beta) = \text{Res}[A(z \rightarrow \beta)]$  and  $\beta = \beta_r + i\beta_i$  is the complex coordinate of the pole. Formula (3) represents a complex wave propagating in the  $\beta_r$  direction whose amplitude attenuates with increasing  $\alpha$  and  $\rho$ , but for  $\alpha \rightarrow \beta_r$  if  $\beta_i \rightarrow 0$ , can be attenuated very little, and can survive even at relatively long distances. As for the phase factor in Eq. (3) we note that, also recovering the time dependence  $\exp(-i\omega t)$ , it exhibits a propagation velocity along a path with the angle  $\alpha$  (phase-path velocity)  $v_{pp}/c = [\cos(\beta_r - \alpha) \cosh \beta_i]^{-1}$  which can be greater or smaller than light velocity  $c$ , the borderline being Eq. (2). We wish to note that, in nondispersive situations (like that of open-air propagation), this result holds true also for the group-path velocity. Indeed, in Ref. [9], experimental results showing superluminal behavior in pulse delay measurements were interpreted in terms of a couple of complex waves [12], a simplified model that can explain the essential features of the experiment. The physical reality is, however, more complicated, since an important role is played also by the "normal" contribution, and the resulting scheme is almost the same one adopted in the optical experiment of Ref. [6], which demonstrates the *X*-shaped waves.

We measured the field amplitude, in the near-field region, emitted by a pyramidal horn fed by a generator in the *X* band at a frequency  $\nu \approx 10$  GHz. The field amplitude was detected by an open-end waveguide connected to the receiver, as a function of the displacement  $l$ , for several values of the

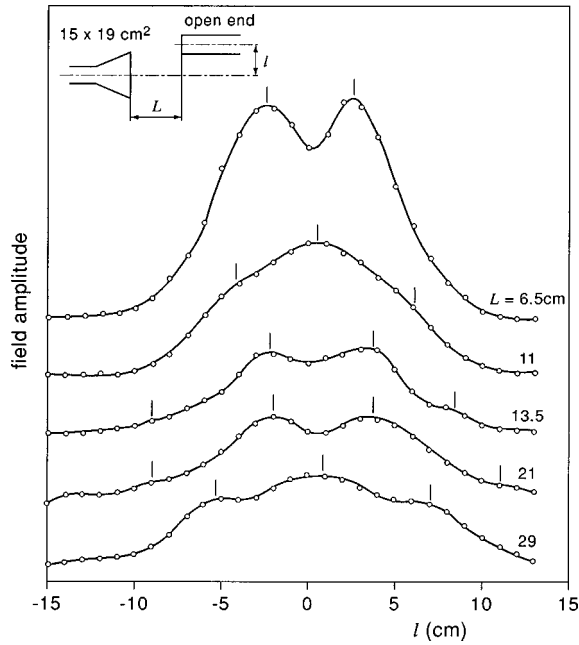


FIG. 1. Structured field amplitude, emitted by a pyramidal horn (flare angle of  $30^\circ$ ) at  $\sim 10$  GHz, detected by an open-end waveguide ( $X$  band), as a function of displacement  $l$  (in the  $H$  plane) for several values of the distance  $L$ . Vertical bars indicate the peak positions of the structure.

distance  $L$ . The results are shown in Fig. 1, and display a structure that is characteristic of interference processes. For greater values of  $L$  ( $\geq 30$  cm) this structure is less evident and tends to disappear. The alternating of maxima and minima at nearly the same value of  $l$ , for different  $L$ , suggests that the interference of at least three waves has to be considered. In fact, the interference of only two plane waves of the same amplitude  $A$ , propagating with angles  $\pm \theta$  with respect to the  $L$  axis, gives rise to an amplitude function  $v = v_1 + v_2 = 2A \exp(ikL \cos \theta) \cos(kl \sin \theta)$  with maxima and minima of the  $|v|^2$  intensity placed at constant positions along the  $l$  coordinate, with a period  $p = \lambda/2 \sin \theta$ . By adding a third wave  $v_3 = B \exp(ikL)$  we obtain an amplitude function

$$V = v + v_3 = \exp(ikL \cos \theta) \{ 2A \cos(kl \sin \theta) + B \exp[ikL(1 - \cos \theta)] \}, \quad (4)$$

which exhibits maxima and minima along the  $l$  coordinate with a period, in the amplitude as well as in the intensity  $|V|^2$ , that is twice as large as the previous one, that is,  $p = \lambda/\sin \theta$ . More important, the maxima and the minima change position by varying  $L$  with a period  $p_1 \approx \lambda/(1 - \cos \theta)$ . This behavior is shown in Fig. 2, which qualitatively reproduces the experimental results of Fig. 1 by identifying the real angle  $\theta$  with  $\beta_r$  of Eq. (3). For evaluating the patterns of Fig. 2, we also introduced a suitable factor into the expression (3): That is, we multiplied  $A$  by  $\exp[k(L \sin \theta + |l| \cos \theta) \sinh \theta_i]$ , where  $\theta_i$ , the imaginary part of  $\theta$  when it becomes complex, has a negative value of a few degrees. (A factor  $\cosh \theta_i$ , which should multiply  $\cos \theta$  and  $\sin \theta$ , can be disregarded). A fitting of this model over the experimental results can be done as follows. In Fig. 3 we place the posi-

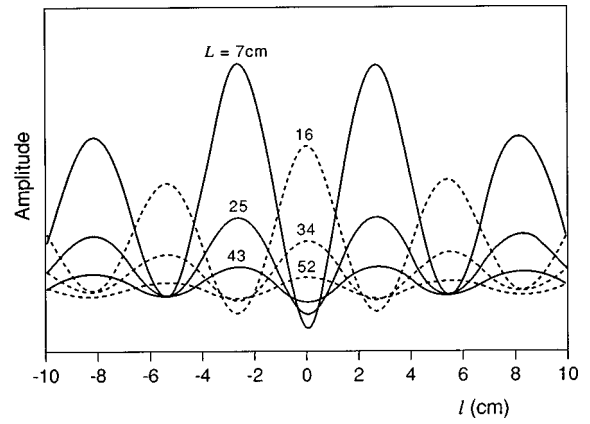


FIG. 2. Amplitude function, as results from the interference of three waves, evaluated as the absolute value of Eq. (4) for  $\theta = 0.6$  ( $\approx 34^\circ$ ),  $k = 2\pi/\lambda = 2 \text{ cm}^{-1}$ ,  $B = 4$ ,  $A = A_0 \exp[k(L \sin \theta + |l| \cos \theta) \sinh \theta_i]$ , with  $A_0 = 1$ ,  $\theta_i = -0.05$  ( $\approx -3^\circ$ ). The amplitude vs  $l$  shows a peaked structure with a period  $p = \lambda/\sin \theta = 5.7$  cm. The positions of the peaks change with  $L$  with a period  $p_1 \approx \lambda/(1 - \cos \theta) \approx 18$  cm.

tions of the peaks of Fig. 1 in the  $(l, L)$  plane. In the same plane, we represent a system of wave fronts that, according to the above analysis, are expressed, as couples of tilted segments, as

$$l = \pm \cot \theta \left( L - \frac{n\lambda}{\cos \theta} - L_0 \right), \quad n = 0, 1, 2, \dots \quad (5)$$

This system of wave fronts appears as a mesh in which each knot corresponds to a maximum of the field intensity  $|V|^2$ . The wave fronts of the “normal” contribution are approximated, also in same Fig. 3, by vertical segments  $\lambda$  spaced. When they coincide exactly with the knots of the tilted wave fronts, Eq. (5), the peaks of the intensity are enhanced. A reasonable fit of the observed peaks is obtained with  $\theta$  ( $\equiv \beta_r$ )  $\approx \pm 30^\circ$ .

Our wave system is substantially the same as that of the optical experiment of Ref. [6], where there is the interference of Bessel  $X$  waves and a plane wave. There, the axial symmetry is obtained with an annular slit, exciting the  $X$  wave, and a concentric pinhole for the plane wave. In our case, this axial symmetry is lacking, and our wave scheme refers only to the  $\eta$  ( $\equiv l$ )  $\xi$  ( $\equiv L$ ) plane, since in the analysis we assumed an infinite size for the exciting aperture along the  $\zeta$  axis. However, any real system has finite size and the observed behavior in the  $(\eta, \xi)$  plane could be extended to each plane containing the  $\xi$  axis. So, we can conclude that also our results can give evidence of  $X$ -shaped waves. The superluminal nature of these waves arises from the  $\cos \theta$  dependence in Eq. (5), which makes the phase velocity equal to  $c/\cos \theta$ . From the results of Fig. 3, we obtained a velocity 15% greater than  $c$ . Higher velocities were demonstrated in Ref. [9] when  $\alpha \neq 0$  directions were considered: the effect increases as  $\cos(\beta_r - \alpha)$  and, for  $\alpha \approx \pm 25^\circ$ , we observed an increase in the velocity of up to  $\sim 40\%$ . However, such an effect tends to disappear for distances of the order of one (for a wavelength of 3 cm) or a few (for a wavelength of the order of 10 cm) meters, that is, within the near-field limit conventionally defined by  $R = 2D^2/\lambda$ , where  $D$  is the width

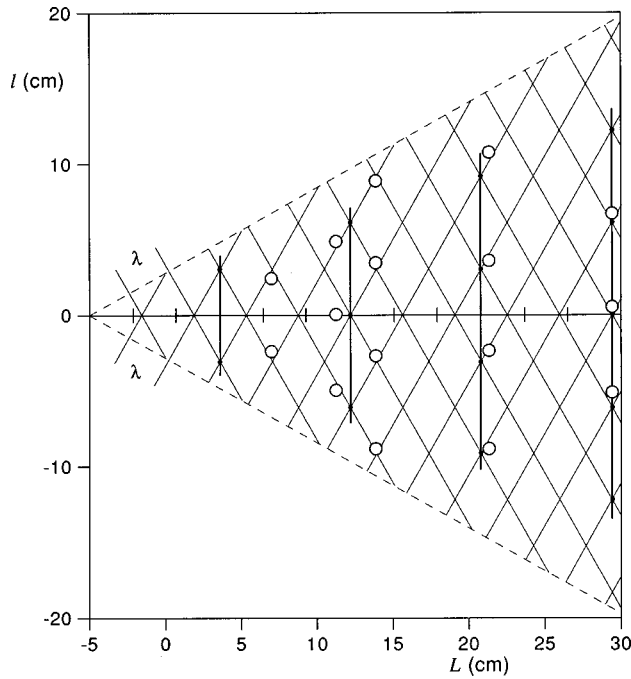


FIG. 3. The peak positions of Fig. 1 are indicated by circles in the  $(L, l)$  plane. They almost coincide with the knots of the mesh of the wavefronts derived from Eq. (5) with  $\lambda=3$  cm,  $\theta(\equiv\beta_r)=30^\circ$ , and  $L_0=-2$  cm. The dashed lines roughly fix the boundaries of the field. The wave fronts of the “normal” contribution are approximated by vertical segments  $\lambda$  spaced: only those that coincide with the knots of the tilted wave fronts are shown. This represents the experimental evidence of X-like waves at microwave scale and their superluminal behavior. When  $L$  increases by 18 cm, the tilted waves are one wavelength in advance with respect to the “normal” wave.

of the launcher aperture and  $\lambda$  the wavelength [see Table I in Ref. [9(b)]]. For a fixed  $D$ ,  $R$  increases with decreasing  $\lambda$ , however, since  $D$  is typically a number of  $\lambda$ ,  $R$  actually increases at longer wavelengths provided that  $D$  is properly augmented.

### III. ZENNECK WAVES

We now reconsider the question posed in the Introduction regarding the possibility of observing superluminal behavior over longer distances, let us say over hundreds of meters or more.

To this purpose, an old long-debated question is related to the presence or not of Zenneck waves (a type of fast wave) in the surface wave of broadcasting [13]. Here, we are not interested in searching for a definitive answer to this question. Rather, assuming that such waves can exist (in that case, the question is how to excite them), we wish to explore the possibility of observing superluminal behaviors at radio frequencies. Let us consider a system consisting of an antenna placed over a flat ground in the presence of finite losses due to the noninfinite conductivity of the Earth plane. In these conditions, the wave fronts are not perpendicular to the ground, due to an electric-field component along the surface, and their inclination produces an increase in the phase velocity along the interface between Earth and air. In general, a wave of this type will give rise to both a reflected and a

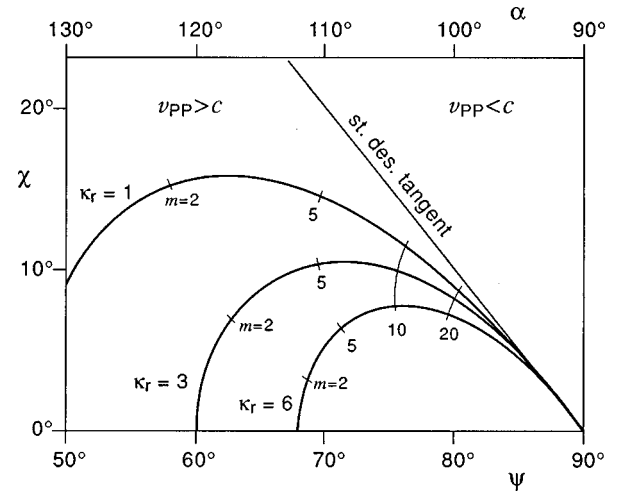


FIG. 4. Loci of the Zenneck-wave pole in the  $(\psi, \chi)$  plane, for different values of the relative permittivity  $\kappa_r$ , as a function of the parameter  $m = \sigma_1 / \omega \kappa_0$ . When the conductivity  $\sigma_1 \rightarrow \infty$ , the curves tend asymptotically to the tangent of the steepest-descent path, but they are always situated on the  $v_{pp} > c$  side. The scale of the observation angle  $\alpha$  is also shown.

transmitted wave entering the Earth plane; however, for a critical value of the incidence angle (the Brewster angle), there is no reflected wave. This condition (required for the existence of Zenneck waves) is verified when, by denoting by  $\psi$  the angle of incidence and by  $\chi$  its imaginary part, we have [13]

$$\tan(\psi - i\chi) = \sqrt{\kappa_r - im}, \tag{6}$$

where  $\kappa_r = \kappa_1 / \kappa_0$  is the relative permittivity of the Earth (medium 1) with respect to air (medium 0) and  $m$

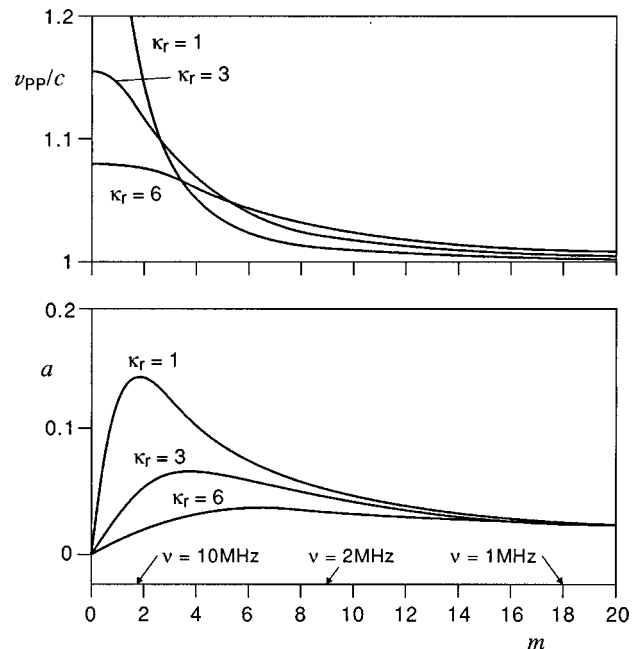


FIG. 5. Phase-path velocity  $v_{pp}/c$  (upper curves) and attenuation constant  $a$  (lower curves) for the Zenneck waves as a function of  $m$  for different values of  $\kappa_r$ . The values, for  $\sigma_1 = 10^{-3}$  mho/m, that correspond to frequencies of 1, 2, and 10 MHz are indicated.

$=\sigma_1/\omega\kappa_0$ ;  $\sigma_1$  is the conductivity of the Earth and  $\omega=2\pi\nu$  is the angular frequency of the wave. The locus of the Zenneck-wave pole, that is, Eq. (6), is represented in the  $(\psi, \chi)$  plane in Fig. 4, for different values of  $\kappa_r$ . In each curve, parameter  $m$  varies from zero (on the left) to infinity when the curves tend asymptotically to the straight line crossing the abscissa at  $\psi=90^\circ$ . The latter represents the tangent to the steepest-descent path, Eq. (2), for an angle of observation  $\alpha=90^\circ$ , that is, that of an observer staying over the Earth plane: this is the extreme position of the steepest-descent path. The Zenneck pole is always situated beyond; therefore, it is never captured by the path deformation as evidenced in Fig. 4 where the Zenneck pole is situated at  $\alpha$  values greater than  $90^\circ$  — the extreme angle of observation — that is, penetrating the ground [11]. It, however, contributes in the steepest-descent representation as a correction term that is significant if the pole is not too far from the steepest-descent path [14].

The analysis of the propagation velocity and of the attenuation factor of the Zenneck-wave contribution is exactly the same as that reported above for the complex waves. In particular, by identifying the angle of incidence  $\psi$  with  $90-\beta_r$  and  $\chi$  with  $\beta_i$  in (3), the phase path velocity is given by  $v_{pp}/c=(\sin\psi/\cosh\chi)^{-1}$  and the attenuation factor, multiplying  $k\rho$  in the same expression (3), is  $a=\cos\psi/\sinh\chi$ . These quantities are represented in Fig. 5 as a function of  $m$  for different values of  $\kappa_r$ . Taking for the Earth's constants the values relative to a "poor ground" [15]:  $\sigma_1=10^{-3}$  mho/m,  $\kappa_r=5$ , ( $\kappa_0=8.84\times 10^{-12}$  F/m),  $m$  ranges from  $\sim 2$  at  $\nu=10$  MHz ( $\lambda=30$  m) to  $\sim 20$  at  $\nu=1$  MHz ( $\lambda$

$=300$  m). At the lowest values of  $m$ , we should obtain superluminal velocity up to  $\sim 10\%$  faster than light and with moderate attenuation ( $a\lesssim 0.05$ ), so as to make this behavior observable also for distances of several wavelengths, exactly as in the microwave experiment described above. In this situation, however, the involved distances should be of the order of hundreds of meters or more, even if the smallness of the effect makes detection difficult.

We can conclude, therefore, that, in the hypothesis that the Zenneck waves can be properly excited [16], superluminal behaviors could be observed even at radio frequencies and explained on the basis of the same mechanism that governs the microwave experiments. Moreover, we wish to note that superluminal behaviors come to be understood even in situations different from those considered here and pose no essential problems for the physics [17,18].

The novelty of this work lies in the fact that we are no longer dealing with true evanescent waves — which disappear over distances of the order of the wavelength — but rather with complex waves that can survive up to distances of several wavelengths, distances that at radio frequencies could reach remarkable values.

In this paper we have analyzed phase-path velocities, and not group-path velocity. However, in nondispersive media, or in the presence of moderate dispersions such as the situation considered here, the two velocities tend to coincide. Our results can therefore be extended also to group velocity, while the controversial question as to whether these results can be extended to signal velocity remains open.

- 
- [1] A. Enders and G. Nimtz, *J. Phys. I* **2**, 1693 (1992).  
 [2] A.M. Steinberg, P.G. Kwiat, and R.Y. Chiao, *Phys. Rev. Lett.* **71**, 708 (1993).  
 [3] Ch. Spielman, R. Szipöcs, A. Stingl, and F. Krausz, *Phys. Rev. Lett.* **73**, 2308 (1994).  
 [4] D. Mugnai, A. Ranfagni, and L.S. Schulman, *Phys. Rev. E* **55**, 3593 (1997).  
 [5] Ph. Balcou and L. Dutriaux, *Phys. Rev. Lett.* **78**, 851 (1997).  
 [6] P. Saari and K. Reivelt, *Phys. Rev. Lett.* **79**, 4135 (1997).  
 [7] R.W. Ziolkowski, D.K. Lewis, and B.D. Cook, *Phys. Rev. Lett.* **62**, 147 (1989).  
 [8] E. Recami, *Riv. Nuovo Cimento* **9**, 1 (1986), and references therein; *Physica A* (to be published).  
 [9] (a) A. Ranfagni, P. Fabeni, G.P. Pazzi, and D. Mugnai, *Phys. Rev. E* **48**, 1453 (1993); (b) A. Ranfagni and D. Mugnai, *ibid.* **54**, 5692 (1996).  
 [10] J. Zenneck, *Ann. Phys. (Leipzig)* **23**, 846 (1907).  
 [11] T. Tamir and A.A. Oliner, *Proc. IEE (London)* **110**, 310 (1963).  
 [12] In the first paper of Ref. [9] these waves were referred to as "leaky waves"; this name is usually attributed, however, to complex waves that exhibit an opposite amplitude behavior (that is, not attenuating but rather increasing up to a given extent), and do not comply with the radiation condition.  
 [13] H.M. Barlow and A.L. Cullen, *Proc. IEE (London)* **100**, 329 (1953).  
 [14] The evaluation of this contribution can be made along the lines of the analysis reported in L.B. Felsen and N. Marcuvitz, *Radiation and Scattering of Waves* (Prentice-Hall, Englewood Cliffs, NJ, 1973), p. 399. It seems, however, that, depending on the analytical expression of  $A(z)$  in Eq. (1), the pole contribution — even if the pole is not properly captured by the integration path — could be the dominant one up to distances of several wavelengths, for angles of incidence  $\psi$  near to  $90^\circ$ .  
 [15] F.E. Terman, *Electronic and Radio Engineering* (McGraw-Hill, New York, 1955), p. 808.  
 [16] The existence of Zenneck waves is only one possibility for obtaining superluminal behavior: we do not exclude, however, that other ways could be considered.  
 [17] See, for instance, Y. Japha, G. Kurizki, *Phys. Rev. A* **53**, 586 (1996).  
 [18] D. Mugnai, A. Ranfagni, and L. Ronchi, *Phys. Lett. A* (to be published); *Atti Fond. Giorgio Ronchi* (to be published).